

Predicting Cumulative Galvanic Corrosion Damage in Aircraft Structures

Robert Adey, Andres Peratta, John Baynham

CM BEASY Ltd
Ashurst Lodge Southampton, SO40 7AA
UK

r.adey@beasy.com

Thomas Curtin

Computational Mechanics International Inc.
25 Bridge Street, Billerica, MA 01821
USA

tcurtin@beasy.com

ABSTRACT

Material degradation mechanisms such as galvanic, pitting, crevice, and intergranular corrosion limit the operational lifetime of aircraft and result in unsustainable long term maintenance costs. Recent studies of naval aircraft suggest that galvanic corrosion is the primary corrosion mechanism, in nearly 80% of the cases, when corrosion damage is observed on the aircraft. Corrosion maintenance is often very labor intensive so more effective scheduling can reduce costs; there is an economical need to move from a “Find and Fix” approach to a more efficient and cost-effective “Predict and Prevent” approach.

A new approach to predicting corrosion damage using computer simulation models is presented where not only the corrosion rate can be predicted for complex multi material structures but also the cumulative corrosion damage to structure experiences during its service life. A demonstration of this new methodology (corrosion Service Life Model) is presented using actual environmental exposure data collected onboard a naval vessel. The effects of crevice and pitting corrosion can also be included in this predictive model. The approach is applicable not only to aircraft but to a wide range of structures subject to atmospheric corrosion

1.0 INTRODUCTION

The annual cost of corrosion for Navy and Marine Corps aviation is estimated at \$3.4 B, accounting for 27.9% of the total maintenance budget, with annual non-availability due to corrosion at 228,471 days [1]. Corrosion maintenance is often very labor intensive so more effective scheduling can reduce costs; there is an economical need to move from a “Find and Fix” approach to a more efficient and cost-effective “Predict and Prevent” approach.

Aircraft are exposed to a wide range of environmental conditions over their operational life and this influences the type and severity of corrosion damage they experience. For example, sea based aircraft experience a much more aggressive, salt-laden, environment than land based aircraft. In order to make meaningful predictions of cumulative corrosion damage it is critical to know the environmental exposure of an aircraft over the course of its lifetime.

Corrosion damage often drives other failure mechanisms including cracks that initiate from the corroded surface

morphology. This is a complicated mechanism where both environmental and mechanical loading contribute to the nature and aggressiveness of the structural damage. Structural integrity decision making is intimately connected to a better understanding of how galvanic corrosion influences the formation of corrosion pits and the initiation of cracks. Use of better design principles will reduce the impact of galvanic corrosion and yield more durable structures.

Recent advancements in computational corrosion modeling tools have the potential to dramatically improve the durability of aircraft by providing engineers with predictive tools to improve material selection and develop more corrosion resistant designs. Corrosion modeling also provides engineers with forecasting tools that can be used to gain insight into the effect of long term corrosion damage; ultimately helping to improve maintenance scheduling and reduce fleet maintenance costs.

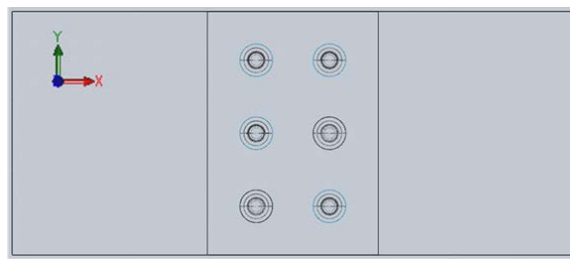
2.0 PREDICTIVE CORROSION MODELING TOOLS

Computational modeling is now widely used in many industries to predict corrosion risk, and to design and help better understand the performance of mitigation measures, including cathodic protection. [[4], [5]]. The Finite Element Method (FEM) has been widely applied as the modeling method in this regard. In this work a modified version of the Nernst-Planck mass transport equation is used to model galvanic behavior. Electroneutrality in the corrosion system (i.e. no charge separation in electrolyte) is assumed along with no bulk motion of the fluid (i.e. fluid velocity = 0). The concentration gradient contribution is also assumed to be much smaller relative to the migration component of the current density. By ignoring these changes in solution chemistry and ion species diffusion the Laplace Equation can be used to model the steady-state current and potential distributions under both bulk and thin film electrolyte conditions.

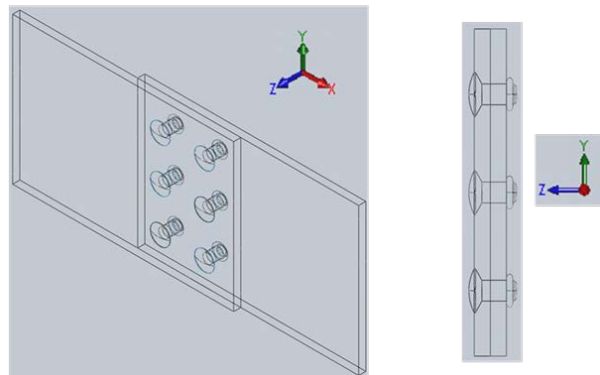
Driven primarily by needs in the aerospace industry, the BEASY Corrosion Manager Software package has recently been improved to include an extended electrochemical database and new analytical tools (i.e. kinetics reaction fitting, curve crossing), support for cumulative corrosion damage predictions, and a connection to an empirically based corrosion pitting model (Figure 1).

This suite of software tools supports a range of sophistication in the prediction of corrosion rates for both bulk (deep electrolyte) and thin-film (atmospheric) electrolytes. The most significant development however, is the ability to make estimates of metal loss for dynamically changing exposure conditions, while also including the geometric effects of the galvanic assembly.

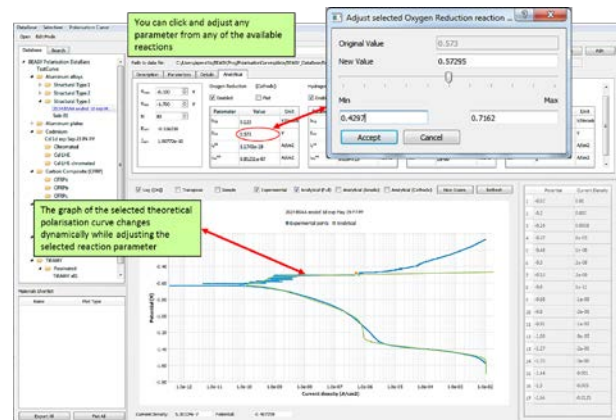
In order to validate the approach an experimental program was developed with the objective of quantitatively understanding the effects of important external variables on the potential and current distributions in the galvanic coupling between SS316 and AA7075-T6 under both immersion and thin-film electrolyte conditions. Of particular interest was the polarization data required to accurately simulate the anodic and cathodic current density under thin film conditions. The successful validation of the computational modeling approach using galvanic sensor measurements will facilitate the development of better corrosion prediction tools. This work also establishes the bases for creating corrosion prediction models that use real time sensor input.



Plates: AA 7075-T6
Rivets: Cadmium plated carbon steel



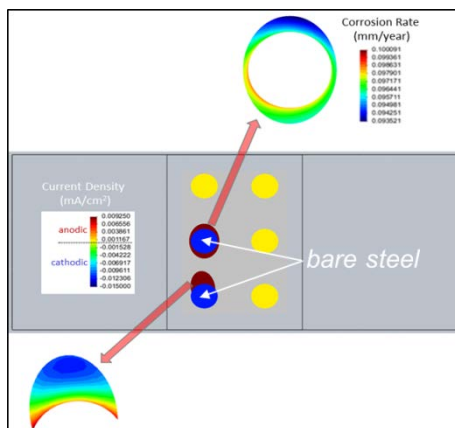
CAD Model Of The Structure



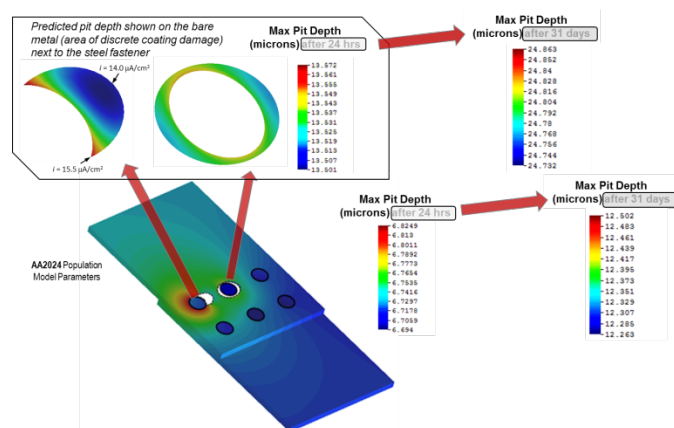
Polarization Database & Curve Crossing Tools

Group	Name	Population	Surface	Net current	Mass Loss	Most positive	Most negative	Max Current	Max Current	Max Corrosion	Max Corrosion	Accumulated	Severity
1	Plate_Top_Switch_BOTTOM	AA7075_Corrosion	0.000336	0.00002943	0.000336	-0.000336	-0.000336	34.036	1.3958	37.316	1.5307	0.48868	0
2	Plate_Top_Switch_Under_Plate	AA7075_Corrosion	5.60364e-05	0.00001733	0.0001733	-0.0001733	-0.0001733	11.8205	7.3871	11.8499	6.3707	0.28811	0
3	Plate_Top_Switch_Under_Plate	Titanium_30_NiFlow	5.60364e-05	-0.0000003	0	0.0000003	-0.0000003	-10.8279	0	0	0	0	0
4	Plate_Top_Switch_BOTTOM	AA7075_Corrosion	0.0000107	0.00000376	0.0000376	-0.0000376	-0.0000376	7.0981	0.000056	7.1777	0.00079	0.00026	0
5	Screen_Shield_01_BOTTOM	Titanium_30_NiFlow	0.0232e-05	-0.00000386	0	0.00000386	-0.00000386	-11.8823	-18.4056	0	0	0	0
6	Screen_Shield_01_BOTTOM	Titanium_30_NiFlow	0.0232e-05	-0.00000386	0	0.00000386	-0.00000386	-11.8823	-18.4056	0	0	0	0
7	Screen_Shield_01_BOTTOM	AA7075_Corrosion	0.0023824	0.113678	1.0005	-0.0043425	-0.0043425	84.84	52.3473	85.8839	37.7888	1.2888	0
8	Screen_Shield_01_TOP	Titanium_30_NiFlow	0.0023824	-0.113678	0	0.0043425	0.0043425	-27.0786	-52.3474	0	0	0	0
9	Screen_Shield_02_BOTTOM	Titanium_30_NiFlow	0.00001408	-0.00000273	0	0.00000273	-0.00000273	-17.7992	-15.2211	0	0	0	0
10	Screen_Shield_02_TOP	Titanium_30_NiFlow	0.00001408	-0.00000273	0	0.00000273	-0.00000273	-17.7992	-15.2211	0	0	0	0
11	Screen_Shield_03_BOTTOM	Titanium_30_NiFlow	0.00001284	-0.00000003	0	0.00000003	-0.00000003	-7.79628	-1.61538	0	0	0	0
12	Screen_Shield_03_BOTTOM	AA7075_Corrosion	0.00000008	0.000000029	0.000000029	-0.000000029	-0.000000029	11.8205	7.3871	11.8499	6.3707	0.28811	0
13	Screen_Shield_03_TOP	Titanium_30_NiFlow	0.00000008	-0.000000029	0	0.000000029	-0.000000029	-11.8205	-7.3871	0	0	0	0
14	Screen_Shield_04_BOTTOM	AA7075_Corrosion	0.00001107	0.0113704	0.0013704	-0.0013704	-0.0013704	85.8839	52.3473	86.9202	37.7888	1.2888	0
15	Screen_Shield_04_TOP	Titanium_30_NiFlow	0.00001107	-0.0113704	0	0.0013704	0.0013704	-85.8839	-52.3473	0	0	0	0

Summary of the corrosion risk of all the materials in the structure



Corrosion Rate Predictions



Pitting Predictions

Figure 2-1: Predictive tools in the BEASY Corrosion Manager software

3.0 CORROSION RATE AND DISTRIBUTION EXPERIMENTAL VALIDATION

In order to validate the approach an experimental program was developed with the objective of quantitatively understanding the effects of important external variables on the potential and current distributions in the galvanic coupling between SS316 and AA7075-T6 under both immersion and thin-film electrolyte conditions. Of particular interest was the polarization data required to accurately simulate the anodic and cathodic current density under thin film conditions.

3.1 Segmented Electrode Galvanic Sensor

A segmented electrode galvanic sensor was designed and fabricated by Luna Innovations Inc [[3]] to investigate the spatial and temporal variations of galvanic currents during static conditions. The sensor was fabricated from 50.8 mm (2 in) wide plates and sheets of aluminum (AA7075-T6) and stainless steel (SS316) of varying thickness in a simple butt-joint configuration. Thinner segments were included closer to the butt-joint interface where anodic and cathodic current density gradients are expected to be the highest and thus require finer spatial resolution. Three SS316 and five AA7075-T6 segments were included. The thicknesses of the SS316 segments, in order from the furthest to the closest to the butt-joint interface were 12.7 mm (0.5 in), 3.2 mm (0.13 in), and 1.2 mm (0.06 in). The thicknesses of the five AA7075-T6 segments, in order from the furthest to the closest to the butt-joint interface were 12.7 mm (0.5 in), 6.4 mm (0.25 in), 2.3 mm (0.13 in), 1.2 mm (0.06 in), and 1.2 mm (0.06 in). All segments were electrically isolated by a 50 μ m thick prepreg layer.

The segmented galvanic sensor was subject to two different tests to measure the anodic and cathodic current density distributions under varying electrolyte layer thicknesses under static relative humidity (RH) conditions. The static holds were conducted with 2.6M NaCl applied to the sensor surface under 90% RH and 25 °C (in a programmable humidity and temperature cabinet) to ensure minimal evaporation. The electrolyte thicknesses were 1000 μ m, and 80 μ m. The 1000 μ m film was created by placing a silicone gasket around the edge of the sensor to create a reservoir that would also break up the fluid surface tension at the edges.

3.2 Model Description

A computational model of the segmented galvanic sensor was created to predict galvanic currents under both immersion and thin film atmospheric conditions. These results were then compared to the experimental measurements in order to validate the modeling approach and the suitability of the polarization data inputs. The model configuration of interest is shown in Figure 3.2.

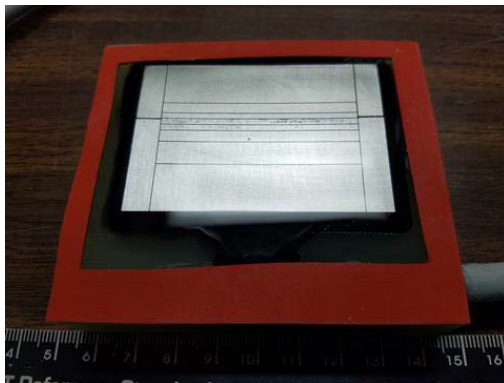


Figure 3-1 Image of segmented electrode sensor, top segments are SS316 and bottom segments are AA7075-T6. Red material is a silicone gasket to create an electrolyte reservoir.

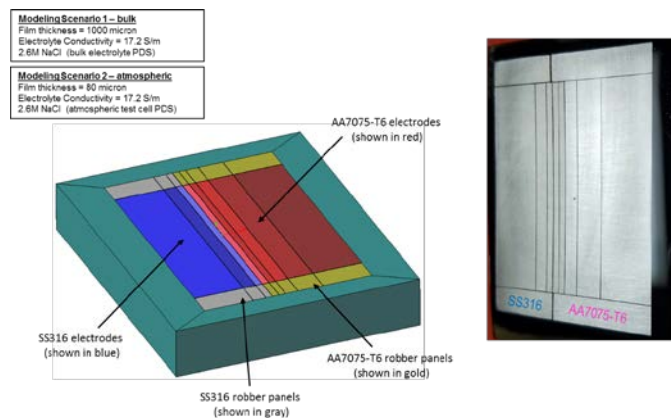


Figure 3-2 Model of Segmented Electrode

The model geometry is first discretized using an appropriate meshing scheme, boundary conditions based on the electrochemical kinetics (i.e. polarization curves) are then applied to represent the SS316 and AA7075 electrodes, and finally the characteristics of the electrolyte film (e.g. conductivity, film thickness) are assigned. The polarization curves, describing the electrochemical kinetics, for both immersion (bulk) and thin-film conditions are shown below in Figure 3-3. In this particular model each electrode is represented as a discrete group of elements so that the total electrode currents can be computed and compared directly to the output from the experimental galvanic sensor (e.g. the interdigitated SS316 and AA7075 electrodes have corresponding element groups in the computational model). Note the total current in the electrode is computed in the computational model by integrating the current density over the surface area of the electrode in contact with the electrolyte.

The computational models were analyzed using electrolyte film thicknesses of 1000 and 80 microns respectively and a uniform conductivity of 17.2 S/m which reflects the molar NaCl concentration of the electrolyte. These film thicknesses were selected to highlight the different galvanic behavior that commonly occurs when a galvanic couple is exposed to immersion compared to thin film conditions.

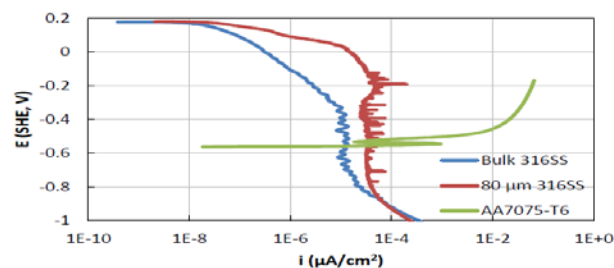


Figure 3-3 Polarization data input for modeling.

3.3 Predicted Corrosion Rate Results

The overall goal of the current modeling work is to quantitatively understand the effects of important external variables (e.g. electrolyte film thickness and conductivity, electrochemical kinetics) on the potential and current distributions in the galvanic coupling between SS316 and AA7075-T6 under different exposure conditions and to validate the methodology against experimental test.

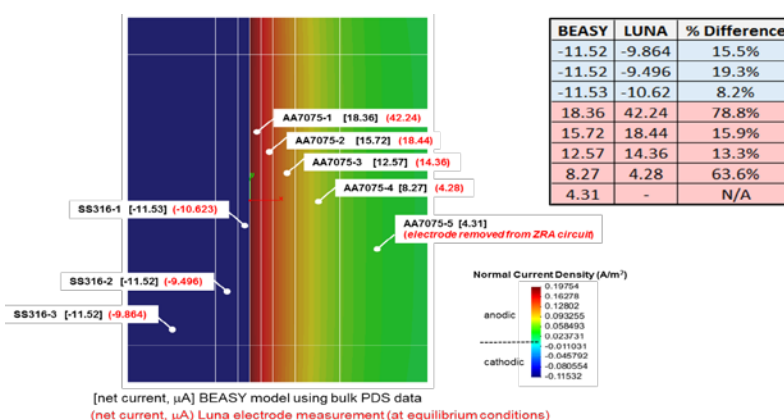


Figure 3-4 Comparison of model predictions with experimental – 1000 micron case.

In Figure 3-4 a comparison is shown of the current in each of the electrodes obtained from the experimental tests and the computational model for the 1000 μm film thickness. On the SS316 electrodes which behave cathodically there is close agreement between the model predictions and the experimental values of the current. The differences in the results range between 8% -19%. On the AA7075 which is behaving anodically, again there is good agreement between the experimental measurements and the model predictions with the differences ranging between 13% and 79% for the significant data. The maximum error is in this case the region very close to the interface between the two materials. This requires further study and possible improvement in the polarization data. However within the context of the overall objectives of the study the results are good and provide validation of the model and the methodology for obtaining the model input data.

In Figure 3-5 a comparison is shown of the current in each of the electrodes obtained from the experimental tests and the computational model for the 80 μm film thickness. In this case the polarization data shown in Figure 3-3 for the 80 μm film is used in the model.

On the SS316 electrodes which behave cathodically there is reasonable agreement between the model predictions and the experimental values of the current. The differences in the results range from 34% to 60%. On the AA7075 which is behaving anodically, there is very good agreement between the experimental measurements and the model predictions with the differences ranging from 1% to 26% if the very small current on electrode 4 is ignored.

Another feature of the results is the close agreement between the model predictions and the experimental measurement of the current distribution over the panels. This suggests that the model is accurately predicting the variation of the current density over the surface geometry. These results therefore provide the basis for predicting a map of the corrosion rate on a structure and the identification of areas with the highest corrosion severity.

Again within the context of the overall objectives of the study the results are good and provide validation of the

model and the methodology for obtaining the model input data.

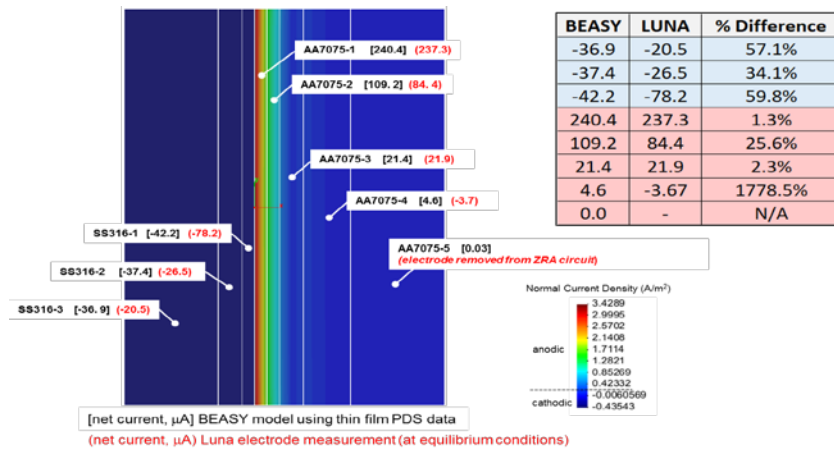


Figure 3-5 Comparison of model predictions with experimental – 80 micron case

The importance of accurately modeling both the thin film resistivity over the structure and the polarization properties under thin film conditions is shown in Figure 3-6 where the current density distribution is shown along the center line of the plates. The dotted red line shows the model prediction for the current density assuming a 1000 μ m film thickness and the black line shows the results for an 80 μ m film thickness. In both cases the full immersion (bulk) polarization data was used in the model and the results show that there is a small increase in the anodic current density for the 80 μ m film. However when polarization data corresponding to the 80 μ m thin film is used in the model the anodic current density and hence the corrosion rate increases by a factor of seventeen.

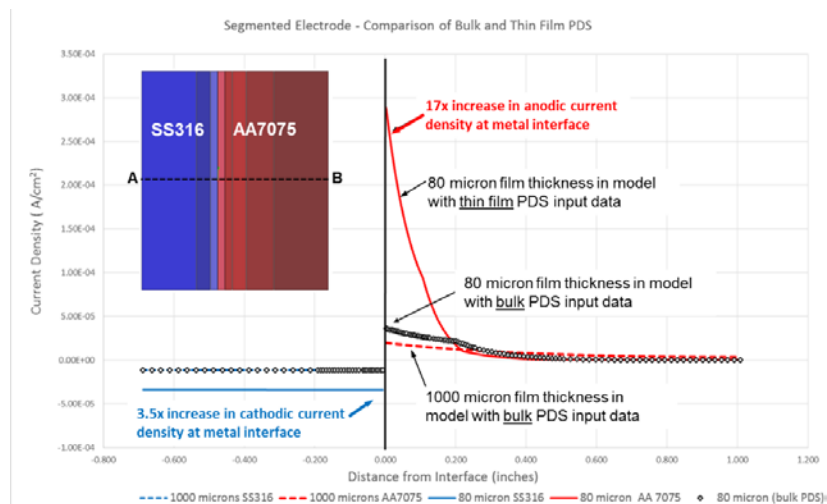


Figure 3-6 PDS Input Requirement – Showing the error introduced when incorrectly using polarization data obtained under full immersion conditions (bulk) for thin film conditions

These tests demonstrate the importance of using the correct input data for the corrosion prediction model particularly for the case where the electrolyte is thin (For example less than 1000 microns) otherwise extremely

misleading results can be obtained

4.0 PREDICTING CUMULATIVE CORROSION DAMAGE

Figure 4-1 illustrates the concept of predicting cumulative corrosion damage. Essentially the requirements are to capture the operational environment history, convert it to a time-based series of computational model input parameters, and predict changes in metal loss and corrosion pitting severity. This approach is, more commonly, referred to as a Corrosion Service Life Model (SLM).

The corrosion SLM is based on the premise of developing an equivalent “flight loading spectrum” for corrosion (or in this case an “environmental loading spectrum”). This approach provides a reasonable first pass at predicting the relative changes in corrosion rate (and ultimately cumulative corrosion damage) for different aircraft usage environments. The approach has the added benefit of being similar to an approach already being used in the aircraft industry (e.g. fracture mechanics based structural lifing). This methodology is generally applicable to other industries where there is a need to predict the cumulative effects of corrosion damage.

The key steps in developing and implementing a Corrosion SLM include:

1. Identifying the environmental exposure history for a particular aircraft platform. Sensor measurements, or the creation of a representative service environment using historical environmental records for example can be used to develop the time-based data needed.
2. Defining the computational model input parameters using the environmental exposure history. The environmental exposure history could be represented by combining several discrete periods where the electrolyte properties may be similar (environmental exposure conditions). These electrolyte properties would, primarily, be determined using laboratory testing methods.
3. Using a time stepping approach (in conjunction with Faraday’s Law) integrate the current density over a discrete time period, to determine the metal loss for each specific environmental exposure condition. Accumulate the metal loss for the given environmental exposure history to determine the cumulative damage over a specified period of time.

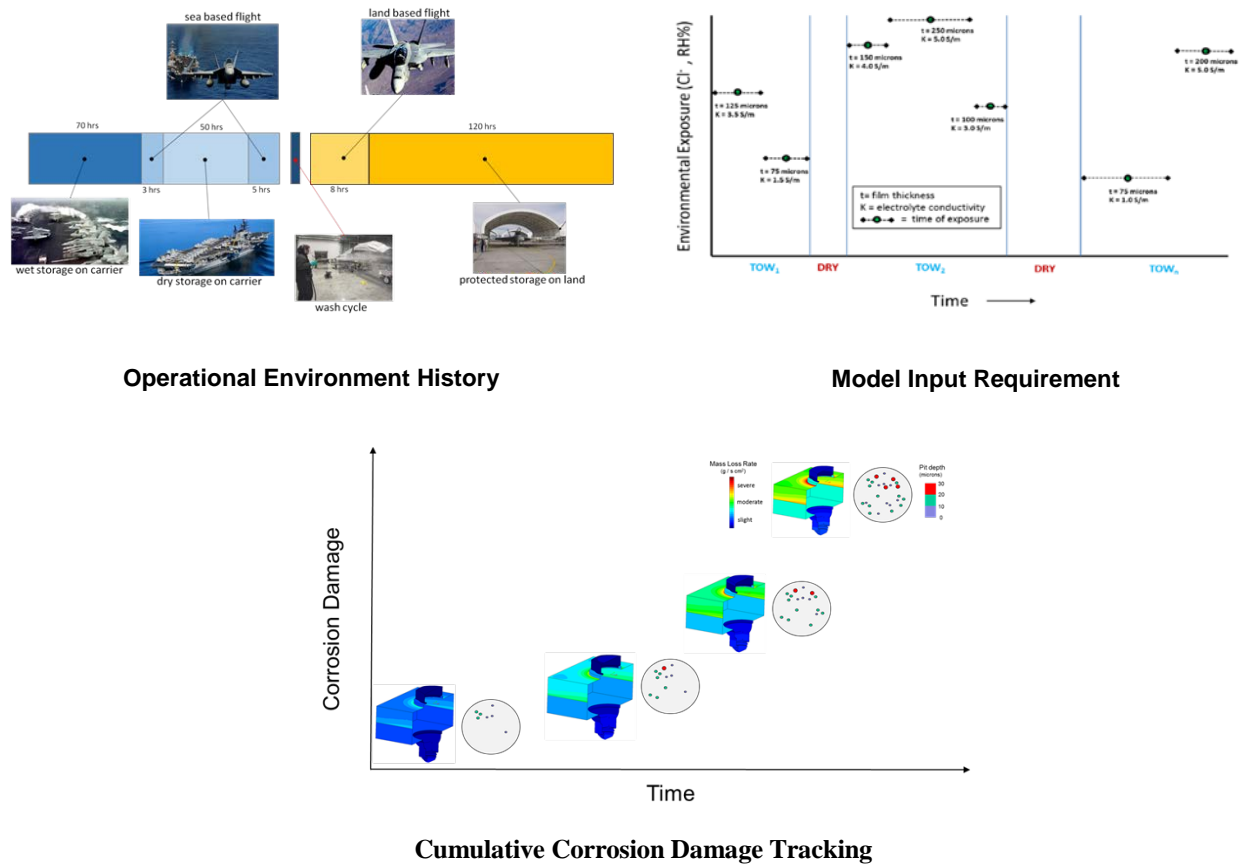


Figure 4-1 Conceptual scheme describing the corrosion Service Life Model

In order to predict the accumulated corrosion damage, the environmental exposure of the structure, over its service life, must be quantifiable. To address this requirement the practicality and feasibility of using corrosion sensor measurements to inform computational models was investigated. This appears to be a more attractive option, compared to using historical environmental records, because the sensor is located directly on the structure and provides an accurate, time-based, measure of the environmental exposure (e.g. T, RH, Rs, Rp).

Sensor measurements and electrochemical laboratory data are used in developing the input requirements for the computational model. Environmental data collected aboard a naval vessel, using a corrosion sensor manufactured by Luna Innovations, was used in our demonstration model. This data was manipulated using an approach, previously developed by NAVAIR [[2]], to characterize the Time of Wetness (TOW) on the metal surface.

The corrosion sensor measurements were further manipulated to refine the surface moisture film classification; characterizing it as WET, SEMI-WET, or DRY. In addition to this TOW (or degree-of-wetness) determination other necessary input parameters for the computational corrosion model include electrolyte properties (conductivity, film thickness) and material specific polarization curves. Polarization curves and conductivity measurements that represent the WET and SEMI-WET conditions were determined in the laboratory. The WET condition is assumed to reflect a bulk electrolyte condition; a 3.5% NaCl solution was used to represent the

electrolyte chemistry. The SEMI-WET condition is assumed to represent more of a thin film condition. A fully saturated solution (36% NaCl) is assumed in this instance. Corrosion is assumed not to occur during the DRY condition.

4.1 Predicting Cumulative Corrosion Damage: A Case Study

An aileron hinge from an F/A-18 aircraft was selected to demonstrate the implementation of the corrosion SLM methodology. The CAD geometry and material properties for the aileron hinge are shown in Figure 4-1. The aileron hinge mounts to the rear and aft spars, and to a connecting rib in the outer wing section.

The model geometry is first discretized with elements using an appropriate meshing scheme. Boundary conditions based on the electrochemical kinetics (i.e. polarization curves) are then applied to represent the various component materials. Lastly, the characteristics of the electrolyte film (e.g. conductivity, film thickness) are assigned.

- Components/Materials
- Aileron Hinge - Aluminium Al-7075
 - Large Fasteners x10 (dia. = 0.4 in) - Stainless Steel 17-4PH
 - Small Fasteners x7 (dia. = 0.3 in) - Stainless Steel 17-4PH
 - Washers - Stainless Steel 17-4PH
 - Pin (dia. = 0.675 in) - Carbon Steel S1020
 - Bushings (x2) - Al-Bronze AMS 4640

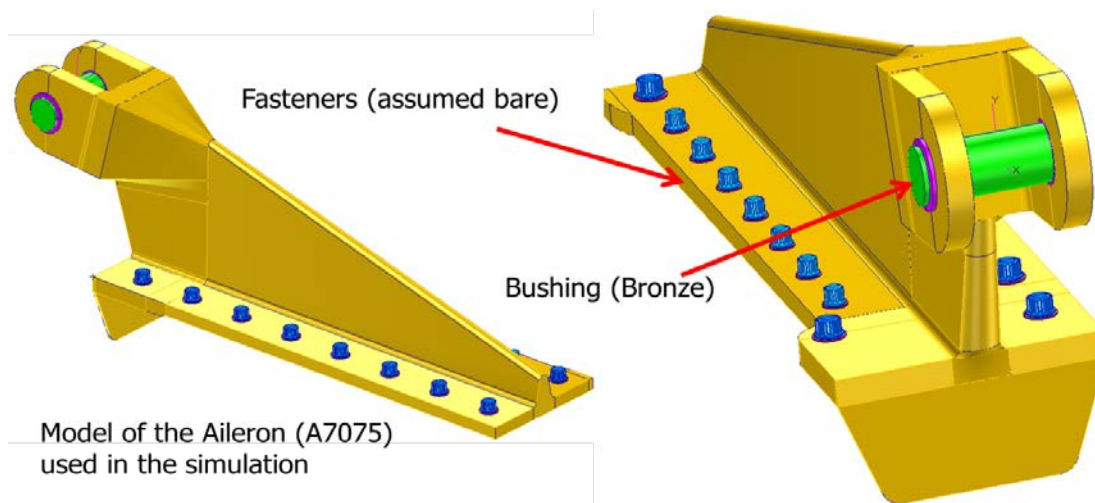


Figure 4-2 CAD model of the aileron hinge used in the corrosion Service Life Model simulation

The electrolyte properties (film thickness, conductivity) used in the model were selected to represent the WET ($t = 500$ microns, $K = 13.41$ S/m) and SEMI-WET ($t = 50$ microns, $K = 66.14$ S/m) conditions. All mating assembly and fastener materials are assumed to be bare metal with the exception of the aileron hinge which is assumed to have a poor quality coating ($R_c = 2 \times 10^4$ ohms/cm²). The steady-state, corrosion rate and potential results, for the two exposure conditions, are shown in Figure 4-2.

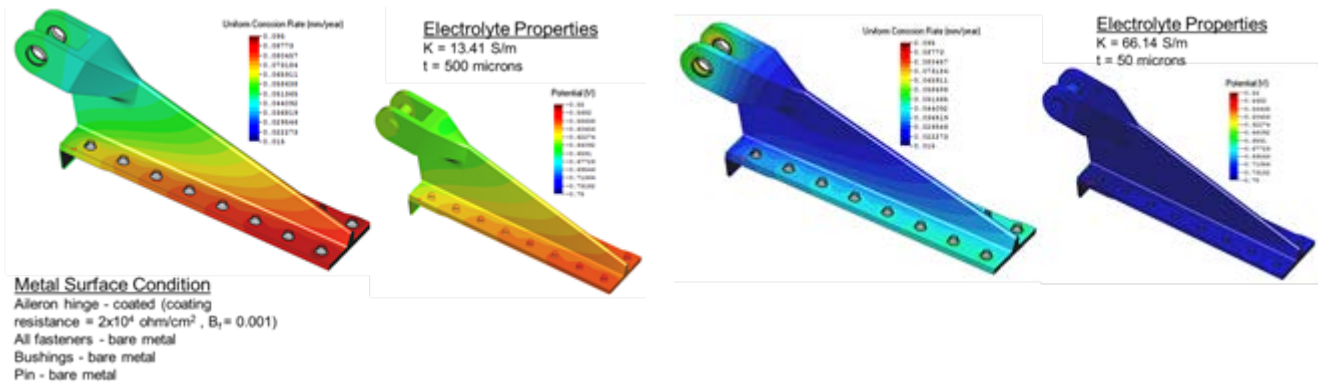


Figure 4-3 Spatial distribution of corrosion rate and potential for the WET exposure condition (3.5% NaCl) (left), and SEMI-WET exposure condition (36% NaCl) (right)

The magnitude and location of peak galvanic stress differs between the two exposure conditions. These differences reflect the complex interaction between the conductivity, film thickness, and polarization curve inputs used in the models. For example the peak galvanic stress occurs around the remote fasteners under the WET exposure condition and at the bushing-lug interface for the SEMI-WET exposure condition.

The cumulative corrosion damage is predicted using the corrosion rates determined from each of the defined exposure conditions (WET, SEMI-WET) in combination with an environmental exposure spectrum. The corrosion damage is determined using Faraday's Law and integrating the corrosion rates over specified time periods. The cumulative corrosion damage is calculated using a time-stepping approach and summing the damage from each discrete exposure period. This concept is illustrated below in Figure 4-3.

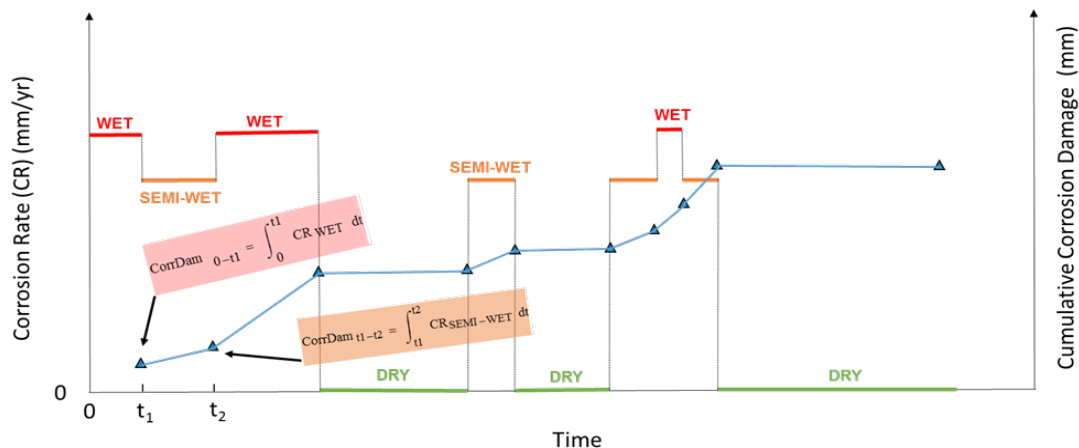


Figure 4-4 Conceptual approach used to predict cumulative corrosion damage

The accumulated corrosion damage (i.e. metal loss) from this simulation is shown in Figure 4-4. The cumulative corrosion damage prediction is made at each element in the computer model to produce a 3D surface contour showing the spatial distribution of corrosion damage for the entire structure.. Although qualitative, the model reflects the general location of the corrosion damage observed in the actual part. The corrosion simulation

predicts high corrosion rates near the bushing and more remote fasteners. Please note that the blue circled areas shown (on the image of the actual part in Figure 4-4) indicate areas where corrosion damage was found during teardown inspection.

CONCLUSIONS

A computational modeling framework has been demonstrated for predicting corrosion rates and cumulative corrosion damage in multi material structures.

Relatively good agreement was obtained between the measured and predicted current density distributions for both immersion and thin film conditions. The computational model accurately captured the spatial distribution of current (i.e. current gradients) measured by a galvanic segmented electrode sensor. The most accurate model predictions of galvanic corrosion under thin film conditions relevant to atmospheric corrosion were obtained when utilizing corrosion kinetic polarization data collected under thin film conditions.

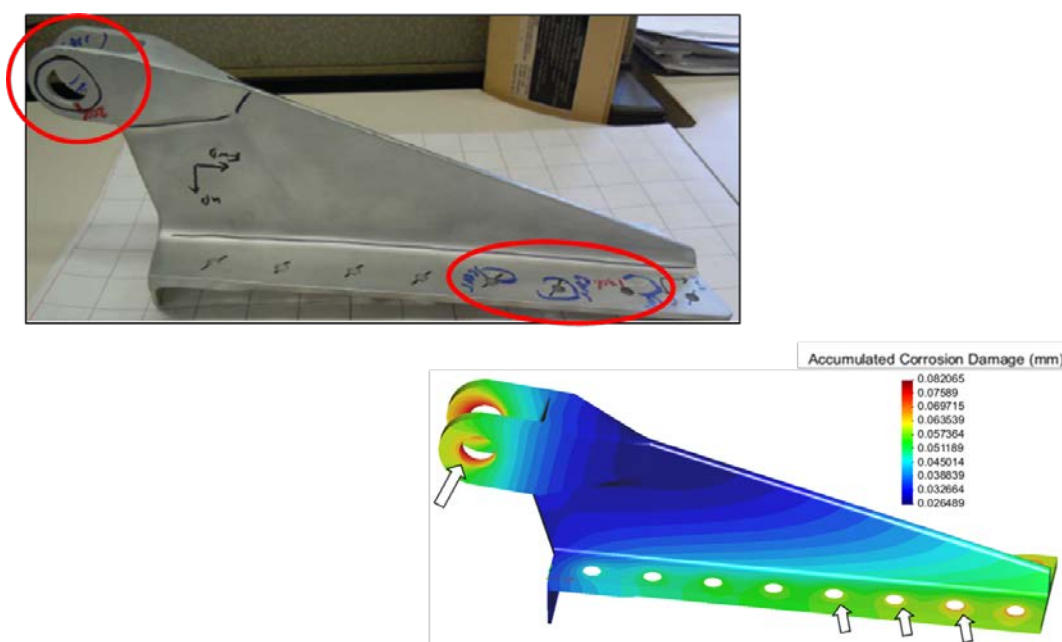


Figure 4-5 Comparison of accumulated corrosion damage

A new methodology (corrosion SLM), capable of predicting the cumulative galvanic corrosion damage for an aircraft component, has been demonstrated. The methodology relies on the creation of an environmental exposure spectrum in this case using corrosion sensor measurement data. A surface moisture classification scheme is applied to the sensor measurements to determine both time-of-wetness and degree-of-wetness. The new corrosion SLM methodology was applied to a multi-material aircraft structure (aileron hinge). The predicted locations of high galvanic stress compared favorably with observations of corrosion damage indicated in a teardown report. This corrosion simulation highlights the importance of considering environmental exposure history, and the geometric effects of a galvanic assembly, when attempting to predict cumulative corrosion damage.

ACKNOWLEDGEMENTS

This research is supported by the ONR Sea Based Aviation Structures & Materials Program, Code 35 Air Warfare and Weapons Department. ONR Technical Point of Contact: William Nickerson

REFERENCES

- [1] <https://www.corrdefense.org/static/media/content/11393.000.00T1-March2018-Ecopy.pdf>.
- [2] C. Boswell-Koller & V. Rodriguez-Santiago. "Corrosion Risk Assessment through Dynamic Environmental Monitoring On Board a Naval Ship", NACE Corrosion Conference 2017.
- [3] Patrick Kramer, Thomas Curtin, Matthew Merrill, Mark Kim, Fritz Friedersdorf, Robert Adey. "Atmospheric Corrosion Measurements to Improve Understanding of Galvanic Corrosion of Aircraft", NACE Corrosion Conference 2018. Denver
- [4] Siva Palani, Theo Hack, Andres Peratta, Robert Adey, John Baynham, Hubertus Lohner. "Modeling Galvanic Corrosion In Multi-Material Aircraft Structures". NACE Corrosion Conference 2013.
- [5] Robert Adey, Cristina Peratta, John Baynham. "How Interference Can Impact The Life Of CP Systems. An FPSO Case Study". NACE Corrosion Conference 2016.

